IEEE Access
Multidisciplinary | Rapid Review | Open Access Journal

Received October 21, 2018, accepted November 10, 2018, date of publication November 21, 2018,
date of current version December 27, 2018.

Digital Object Identifier 10.1109/ACCESS.2018.2882461

Decentralized Optimal Reactive Power Dispatch of Optimally Partitioned Distribution Networks

PEISHUAI LI[1], (Student Member, IEEE), ZAIJUN WU[1], KE MENG[2], GUO CHEN[2], AND ZHAO YANG DONG[2], (Fellow, IEEE)

[1]School of Electrical Engineering, Southeast University, Nanjing 210096, China
[2]School of Electrical Engineering and Telecommunications, University of New South Wales, Sydney, NSW 2052, Australia

Corresponding author: Zaijun Wu (zjwu@seu.edu.cn)

This work was supported in part by the National Natural Science Foundation of China under Grant 51677025, in part by the Fundamental Research Funds for the Central Universities and Research Innovation Program for College Graduates under Grant KYLX16_0209, in part by the State Grid Corporation Project under Grant 52110417000A, and in part by the Australian Research Council under Grant DE160100675.

ABSTRACT This paper proposes a two-stage decentralized optimal reactive power dispatch (D-ORPD) framework, which considers the network partitioning influence in distributed optimization. The first stage is to divide the distribution networks (DNs) into several high-intra-cohesion and low-coupling sub-networks while the mathematical model is constructed based on partition indexes. This optimal partition designation reduces information exchange between adjacent sub-networks. Then, with the reduced information exchange, the distributed computation would be accelerated. Based on the network optimal partition, the D-ORPD model is constructed in a ''decomposition-coordination'' pattern during the second stage. To enhance the consistency between distributed and centralized optimization, the D-ORPD is improved by the proposed virtual load, which simulates the load characteristic of sub-networks. The alternating directions method of the multipliers (ADMM) algorithm is utilized to solve the mathematical model effectively. Moreover, case studies on the PG&E 69 bus test system and the IEEE 123 bus test system are executed by the MATLAB platform to demonstrate the validity and effectiveness of the proposed method.

INDEX TERMS Network partitioning, reactive power dispatch, virtual load, distributed optimization.

I. INTRODUCTION

The integration of distributed generations (DGs) is one of the key features in modern active distribution networks (ADNs). DGs refer to small-scale generation units that are normally located on the consumer's side, such as rooftop solar photovoltaics (PV) and residential wind turbines (WT). These devices provide sustainable electricity generation to supply local demand. Besides, through proper design and scheduling, DGs also can be an excellent resource in reactive power control, which is known as effective in reducing power losses, improving voltage stability, improving power quality, etc. [1]. To realize the control of reactive power optimally, the optimal reactive power dispatch (ORPD) is proposed. Normally, ORPD can be classified into centralized and decentralized frames [2].

Various efforts have been made to solve ORPD and the approaches based on convex relaxation have been researched and utilized widely. Among these convex relaxation methods, second-order cone programming (SOCP) and semidefinite programming (SDP) are representative. In [3] and [4], the SOCP was inverted into solve ORPD problem for distribution networks(DNs) and the exactness of relaxation has been proven under relaxation conditions. In [5], the SDP was utilized to solve non-convex optimization problem and it has been proven that there is no duality gap for exact relaxation. A centralized voltage/var optimization framework was proposed in [6], where the problem was formulated as a mixed-integer programming problem and solved by branch and cut algorithm. In [7], a reactive power compensation system was established, in which the reactive power dispatch devices were controlled in a centralized way.

The works above are all about using centralized approaches to support DNs operation by compensating reactive power. As for the centralized optimal reactive power dispatch (C-ORPD), the system data are collected and conducted by the operation center. According to the high-level penetration of intermittent and fluctuated DGs, DNs are shown as massive controllable devices, complex operating status and flexible operating conditions. Thus, the requirement of communication bandwidth, computation and storage resource increases

sharply along with the expansion of DNs. The traditional centralized optimization is uneconomical and limited in large-scale high renewable-penetrated DNs. The distributed optimization scheme known as high robustness, fast calculation speed and plug-in capability is a good solution to large-scale optimization problem [8]. The alternating direction of method of multipliers (ADMM) is well-established and effective in solving large-scale optimization problem by decomposing the hard-solving original problem into several easy-solving sub-problems. As for its applications in D-ORPD, the original ADMM is utilized for OPF in unbalanced micro-grid [9], optimal reactive power control of DGs in DNs [10], [11] and optimal tap setting for on-load tap changer (OLTC) in DNs [12]. In [13], a fully distributed algorithm was introduced by eliminating the global variable in ADMM. A two-stage D-ORPD architecture which controls reactive power support from local controllers and neighboring controllers was proposed only relying on local information in [14]. Reference [15] proposed a convex distributed approach for OPRD by utilizing a graph to describe the information communication between local controllers.

In D-ORPD, the original centralized problem is decomposed into several sub-problems and this decomposition is corresponding to DNs partitioning. The consistency between D-ORPD and C-ORPD is ensured by the information exchange between adjacent sub-networks. Normally, most researches on D-ORPD only focus on distributed architecture or distributed algorithm without considering the information exchange between sub-networks. However, the speed of distributed calculation is effected by the information exchange [16], [17]. As in [16], it was pointed out that the convergence speed related to the network nodes communication, the number of nodes, desired level of accuracy, etc. Reference [17] illustrated the important influence of communication graph to convergence speed in distributed calculation. Due to the coupling existing in DNs, the information communication between adjacent sub-networks relates much to the DNs partition. Specifically, if the sub-networks are featured of high intra-cohesion and low coupling, the operation state variation inside one sub-network would affect other sub-networks slightly. Therefore, the information exchange between adjacent sub-networks would be rare. On the contrast, if the DNs are portioned into several low intra-cohesion and high coupling sub-networks, it normally needs lots of information exchange during distributed computation. Therefore, the network partitioning is a non-negligible factor in distributed optimization.

For one arbitrary node, the voltage variation caused by reactive power injections from any other nodes could be illustrated by electrical distance (ED), thus ED is one typical networks partitioning standard [18]. K-means clustering algorithm, well-known for cluster analysis in data mining is one heuristic approach and its clustering results are featured of strong similarities in intra-class and weak similarities between inter-class [19], [20]. Thus, K-means is a prominent method in DNs partitioning [20]. In addition, the systematic approach utilizing spectrum [21] and graph-based algorithm [22] are also typical approaches in DNs partitioning.

Considering the influence of information exchange on distributed computation, a novel D-ORPD approach based on DNs partition is proposed. The major contributions are shown as below.

(1) A novel two-stage D-ORPD framework which considers the influence of information communication on distributed computation speed is proposed. In the first stage, the DNs is partitioned optimally to reduce information exchange between neighboring sub-networks. On the basis of the DNs partition, the decentralized ''decomposition-coordination'' optimization architecture is constructed on the second stage.

(2) An optimal DNs partitioning method based on the partition indexes and the binary particle swarm optimization (BPSO) is developed. By applying this method, the original network is divided optimally into several high intra-cohesion and low coupling sub-networks.

(3) The D-ORPD model is improved by utilizing the virtual load to simulate the load characteristic of the sub-networks. This virtual load designation enhances the consistency between centralized optimization and decentralized optimization.

The reminder of the paper is shown as follows. Section II analyzes the coupling features inside DNs and develops the DNs partitioning approaches based on partition indexes and BPSO. The D-ORPD mathematical model is established and solved by ADMM in section III. Section IV shows the case studies and the collusion is drawn in Section V.

II. DISTRIBUTION NETWORK OPTIMAL PARTITION

A. ELECTRICAL DISTANCE

During power flow calculation in Newton-Raphson algorithm, the correlation equation is shown as

$$\begin{bmatrix} \boldsymbol{\Delta\theta} \\ \boldsymbol{\Delta V} \end{bmatrix} = \begin{bmatrix} \mathbf{S}_{\mathbf{P}}^{\boldsymbol{\theta}} & \mathbf{S}_{\mathbf{Q}}^{\boldsymbol{\theta}} \\ \mathbf{S}_{\mathbf{P}}^{\mathbf{V}} & \mathbf{S}_{\mathbf{Q}}^{\mathbf{V}} \end{bmatrix} \begin{bmatrix} \boldsymbol{\Delta P} \\ \boldsymbol{\Delta Q} \end{bmatrix} \tag{1}$$

where, $\boldsymbol{\Delta\theta}$, $\boldsymbol{\Delta V}$, $\boldsymbol{\Delta P}$ and $\boldsymbol{\Delta Q}$ is the variation of voltage angle, voltage magnitude, active power injection and reactive power injection respectively, $\mathbf{S}_{\mathbf{P}}^{\boldsymbol{\theta}}$, $\mathbf{S}_{\mathbf{Q}}^{\boldsymbol{\theta}}$, $\mathbf{S}_{\mathbf{P}}^{\mathbf{V}}$ and $\mathbf{S}_{\mathbf{Q}}^{\mathbf{V}}$ represents the ''voltage phase angle-active power injection'' sensitivity, ''voltage phase angle-reactive power injection'' sensitivity, ''voltage magnitude-active power injection'' and ''voltage magnitude-reactive power injection'' respectively.

The reactive power injection is the only controllable variable in ORPD. Then only the ''voltage magnitude-reactive power injection'' is considered and this sensitivity can be described as

$$\mathbf{S}_{\mathbf{Q}}^{\mathbf{V}} = \partial \mathbf{V} / \partial \mathbf{Q} \tag{2}$$

where, $\mathbf{V}$ is the voltage magnitude vector and $\mathbf{Q}$ is reactive power injection vector.

In power networks, one relationship exists between the voltage magnitude variations of different nodes and this relationship is defined in an attenuation pattern.

The attenuation relationship is shown as

$$\Delta V_i = \partial_{ij} \Delta V_j \tag{3}$$

$$\partial_{ij} = [\frac{\partial V_i}{\partial Q_j}] \Big/ [\frac{\partial V_j}{\partial Q_j}] \tag{4}$$

where, ∂_{ij} is the attenuation parameter between node i and node j, ΔV_i and V_i represents the voltage magnitude variation and voltage magnitude at node i respectively, ΔV_j, V_j and Q_j represents the voltage magnitude variation, voltage magnitude and reactive power injection at node j respectively.

Then, ED is defined as

$$d_{ij} = d_{ji} = -log(\partial_{ij} \cdot \partial_{ji}) \tag{5}$$

where, d_{ij} is the electrical distance between node i and node j.

B. PARTITIONING INDEXES

The ideal partitioning should show strong regional decoupling features, which are close electrical connection inside each sub-network and sparse relationship between different sub-networks. Then, the evaluation indexes of DNs partitioning are constructed based on these regional decoupling features. Referring to [20], four DNs partitioning evaluation indexed are shown as below.

1) INTRA-SUB-NETWORK COHESIVENESS INDEX (ISCI)

The intra-sub-network cohesiveness index (ISCI) shows the degree of intra-cohesion inside each sub-network. The intra-ED is defined to describe the sum of ED between any two buses belonging to the same sub-network. In D-ORPD, ECI is measured by summing the intra-ED for all the sub-networks.

The ISCI is expressed as:

$$ISCI = 1 - \frac{\sum_{i=1}^{n} \sum_{j \in SNi} d_{ij}}{\sum_{i=1}^{n} \sum_{j=1}^{n} d_{ij}} \tag{6}$$

where, SNi represents the subset describing the sub-network containing i.

2) INTER-SUB-NETWORKS DECOUPLING INDEX (ISDI)

The inter-sub-networks decoupling index (ISDI) reflects the sparsity between different sub-networks. And this index is evaluated by ED between the buses which are separated into different sub-networks. ISDI can be expressed as:

$$ISDI = 1 - \frac{\sum_{i=1}^{n} \sum_{j \notin SNi} \frac{1}{d_{ij}}}{\sum_{i=1}^{n} \sum_{i \neq j, j=1}^{n} \frac{1}{d_{ij}}} \tag{7}$$

3) SUB-NETWORKS COUNT INDEX (SCI)

The sub-networks count index (SCI) is utilized to measure the reasonability in the amount of sub-networks divided. Normally, the clustering efficiency, the intra-cohesion and the inter-decoupling are key factors in deciding the amount of sub-networks. However, as DNs are industrial power networks, the communication cost, operation cost and investment should also be considered during networks partitioning. And these two sides of requirement could be met by setting the ideal count of sub-networks approximately and regulate it during processions. The long-normal probability density function is utilized to describe the SCI, shown as:

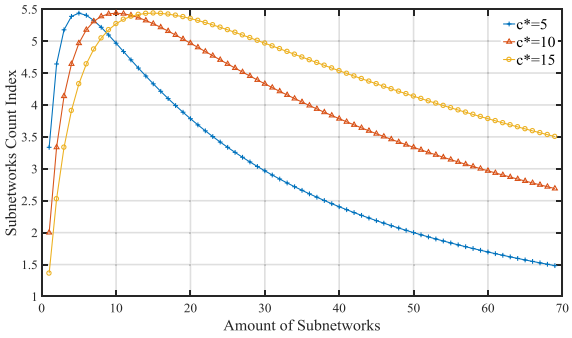

FIGURE 1. Sub-networks count index of PG&E 69 bus test system.

$$SCI = e^{-\frac{(\ln c - \ln c^*)^2}{2\sigma^2}} \tag{8}$$

$$\sigma = w \ln(n) \tag{9}$$

where, c is the count of sub-networks, c^* is the advanced setting count of sub-networks, w is the penalty factor. The SCI of PG&E 69 bus system under different advanced setting count is shown in Fig. 1.

4) PHYSICAL CONNECTION INDEX (PCI)

Different with some other complex networks, there is definite physical connection between nodes in DNs. For each sub-network, all nodes can be linked by branches within itself. Then, to ensure this physical connection after partitioning, the physical connection index (PCI) is constructed. PCI is shown as below.

$$PCI = \begin{cases} 0 & subnet\ worksnot\ fully\ connected \\ 1 & otherwise \end{cases} \tag{10}$$

Based on the above four indexes, the fitness function which evaluates the results of DNs partitioning is constructed as below.

$$Fitness = (w_1 \cdot ISCI + w_2 \cdot ISDI + w_3 \cdot SCI) \cdot PCI \tag{11}$$

where, w_1, w_2 and w_3 reflects the weight of ISCI, ISDI and SCI with $w_1 + w_2 + w_3 = 1$.

C. NETWORKS PARTITIONING ALGORITHM BASED ON BINARY PARTICLE SWARM OPTIMIZATION

1) PARTICLE CODING

In particle swarm optimization (PSO), each particle has the properties as position and velocity while its position represents the possible solution and velocity determines the searching direction. For particle i belonging to the swarm containing

n particles in m dimensions, the coding strategy is shown as below:

$$\boldsymbol{P}_i = [p_{i1}, p_{i2}, \ldots, p_{im}], \quad 1 \le i \le n \tag{12}$$
$$\boldsymbol{V}_i = [v_{i1}, v_{i2}, \ldots, v_{im}], \quad 1 \le i \le n \tag{13}$$
$$\boldsymbol{LP}_i = [lp_{i1}, lp_{i2}, \ldots, lp_{im}], \quad 1 \le i \le n \tag{14}$$
$$\boldsymbol{GP} = [gp_1, gp_2, \ldots, gp_m] \tag{15}$$

where, $\boldsymbol{P}_i$ represents the position of particle i and each element of vector $\boldsymbol{P}_i$ represents the sub-network serial number of the corresponding node, e.g., p_{im} denotes the number of sub-network that node m belongs to. Correspondingly, $\boldsymbol{V}_i$ and $\boldsymbol{LP}_i$ is the velocity and the current optimal position of particle i. $\boldsymbol{GP}$ is the current optimal position of the whole particle swarm.

2) PARTICLE VELOCITY RENEWAL

The particle vector renewal in conventional PSO is used to modify the solution towards the optimum directly during iteration. In DNs partitioning, there is not any explicit formulation for the solution, thus the velocity drives the particle towards through BPSO. Then, the signal function is established as below,

$$sig(x) = \begin{cases} 1 & rand(0,1) < sigmoid(x) \\ 0 & rand(0,1) \ge sigmoid(x) \end{cases} \tag{16}$$
$$sigmoid(x) = \frac{1}{1+e^{-x}} \tag{17}$$

Based on the signal function, the particle velocity renewal strategy is shown as:

$$v_{ik}(t+1) = sig(wv_{ik}(t) + c_1 r_1(p_{ik}(t) \oplus x_{ik}(t)) + c_2 r_2(g_k(t) \oplus x_{ik}(t))) \tag{18}$$
$$1 \le k \le m \tag{19}$$

where, t is the iteration time, w is the inertia weight, c_1 and c_2 are the learning factors, r_1 and r_2 are the speed acceleration coefficients, $\oplus$ reflects the "exclusive or" operation.

3) PARTICLE POSITION RENEWAL

In DNs partitioning, there are two features shown as following. i) the physical connection of nodes assigned in the same sub-network must be ensured, which is in corresponding with PCI; ii) the adjacent nodes always belong to the same or adjacent sub-networks. Based on these two features, the particle position renewal strategy is constructed, shown as below,

$$x_{ik}(t+1) = \begin{cases} x_{ik}(t) & v_{id} = 0 \\ C(rand(d_{\leftrightarrow k})) & v_{id} = 1 \end{cases} \tag{20}$$

where, $d_{\leftrightarrow k}$ represents the nodes linked to node k directly, $C(rand(d_{\leftrightarrow k}))$ represents the sub-network serial number of one random node belonging to the set described by $d_{\leftrightarrow k}$.

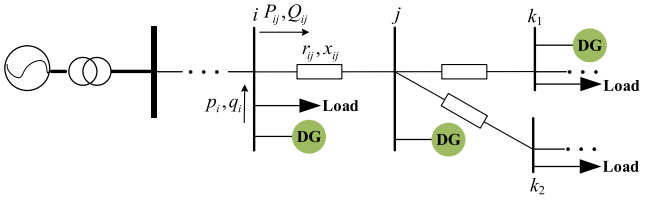

FIGURE 2. Topology of simplified radial distribution network.

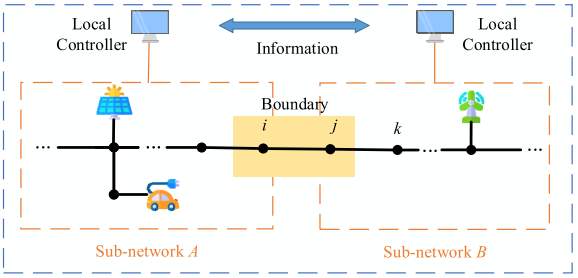

FIGURE 3. Decentralized optimal reactive power dispatch architecture.

III. DECENTRALIZED OPTIMAL REACTIVE POWER DISPATCH MATHEMATICAL MODEL

A. THE MODEL OF DISTRIBUTION NETWORK

The general model of a radial distribution network is shown in Fig. 2. Let $\mathbf{N}$ represent all the nodes and $\widehat{\mathbf{N}}$ represent the nodes except the feeder. For node $i(i \in \mathbf{N})$, s_i, p_i, q_i and V_i denotes the complex power injection, active power injection, reactive power injection and voltage magnitude respectively. The set of all branches is expressed by $\mathbf{E}$, with $(i,j) \in \mathbf{E}$ represents the branch pointing from node i to node j. Let $z_{ij} = r_{ij} + jx_{ij}$ denote the complex impedance, $S_{ij} = P_{ij} + jQ_{ij}$ represent the sending-end complex power, and I_{ij} expresses the complex current. The variable v_i and l_{ij} are inverted for model construction while it exists $v_i = V_i^2$ and $l_{ij} = I_{ij}I_{ij}^* = |I_{ij}|^2$. The set of nodes connecting with DGs is denoted by $\mathbf{N}_{DG}$.

B. DECENTRALIZED OPTIMAL REACTIVE POWER DISPATCH WITH VITURAL LOAD

The D-ORPD mathematical model is constructed in a "decomposition-coordination" architecture, in which the original centralized problem is decomposed into several sub-problems. Each sub-problem is corresponding with each sub-network. The coordination is realized by information communication between any two adjacent sub-networks. The D-ORPD architecture is shown in Fig. 3.

The boundary conditions are utilized to exchange information between adjacent sub-networks. As in Fig. 3, sub-network A connects with sub-network B through the boundary line (i, j). Correspondingly, the boundary conditions are the state variables of the nodes and branch line of the boundary, shown as V_i, V_j, P_{ij}, Q_{ij} and I_{ij}. Then, during the local optimization such as for sub-network A, the node j and line (i, j) also need to be inclusive. It is apparent that the load

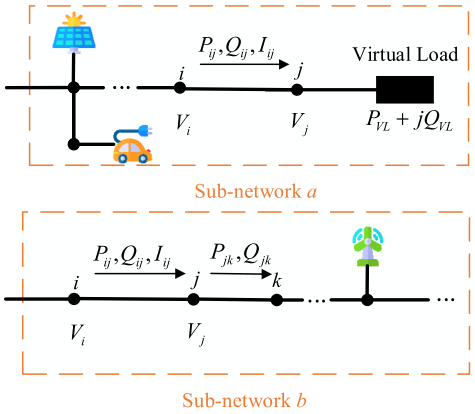

FIGURE 4. The augmented sub-networks with virtual load.

characteristic of the downstream sub-networks is not considered in the previous boundary conditions. However, to guarantee the local optimization for sub-network A being in full accord with the centralized optimization, not only the load at node j, but also the existing active power and reactive power exchange between node j and node k are needed to be considered. These active power and reactive power exchanges reflect the load characteristic of the downstream sub-networks. To describe the necessary load characteristic, the virtual load is proposed in this paper. Thus, applying the virtual load, the consistency of local optimization and centralized optimization is ensured. With the virtual load, the augmented sub-networks are shown in Fig. 4.

Based on above analysis, it can be inferred that the augmented boundary variables for sub-network a is $\mathbf{x}_{ab} = (V_i, V_j, P_{ij}, Q_{ij}, I_{ij}, P^a_{VL}, Q^a_{VL})$ and the boundary variables for sub-network b is $\mathbf{x}_{ba} = (V_i, V_j, P_{ij}, Q_{ij}, I_{ij}, P_{jk}, Q_{jk})$. The auxiliary variable is $\mathbf{u}_{ab} = (\overline{V_i}, \overline{V_j}, \overline{P_{ij}}, \overline{Q_{ij}}, \overline{I_{ij}}, \overline{P_{VL}}, \overline{Q_{VL}})$ and the dual variable λ is inverted to dualize this model. Then, the distributed objective function of sub-network a is shown as

$$L_a(\mathbf{x}_a, \mathbf{u}_a, \boldsymbol{\lambda}_a) = f_a(\mathbf{x}_a) + \sum_{i=1}^{nsa} (\boldsymbol{\lambda}^T_{abi} \cdot (\mathbf{x}_{abi} - \mathbf{u}_{abi}) + \frac{\rho}{2} \|\mathbf{x}_{abi} - \mathbf{u}_{abi}\|_2^2) \quad (21)$$

$$f_a = \sum_{(i,j)\in \mathbf{E}_a} r_{ij} l_{ij} \quad (22)$$

$$\mathbf{u}_a = (\mathbf{u}_{ab1}, \ldots, \mathbf{u}_{abnz}) \quad (23)$$

$$\boldsymbol{\lambda}_a = (\boldsymbol{\lambda}_{ab1}, \ldots, \boldsymbol{\lambda}_{abnz}) \quad (24)$$

where, $\mathbf{E}_a$ is the set of branches for sub-network a with its corresponding boundary conditions, $\mathbf{x}_a$, $\mathbf{u}_a$ and λ_a is the local variable vector, auxiliary variable matrix and dual variable matrix of zone a respectively, ρ is the penalty parameter, nsa is the number of sub-networks connecting with sub-network a.

The mathematical model of D-ORPD is shown as

$$\min \sum_{a=1}^{ns} L_a \quad (25)$$

$$s.t.\ v_j = v_i + (r_{ij}^2 + x_{ij}^2) l_{ij} - 2(r_{ij}P_{ij} + x_{ij}Q_{ij}) \quad \forall (i,j) \in \mathbf{E}_a \quad (26)$$

$$\sum_{(j,k)\in E} P_{jk} - \sum_{(i,j)\in E} (P_{ij} - r_{ij} l_{ij}) = p_j \quad \forall j \in \widehat{\mathbf{N}}_a \quad (27)$$

$$\sum_{(j,k)\in E} Q_{jk} - \sum_{(i,j)\in E} (Q_{ij} - x_{ij} l_{ij}) = q_j \quad \forall j \in \widehat{\mathbf{N}}_a \quad (28)$$

$$q^{\min}_{i,DG} \le q_{i,DG} \le q^{\max}_{i,DG} \quad \forall i \in \mathbf{N}_{DG,a} \quad (29)$$

$$(V_i^{\min})^2 \le v_i \le (V_i^{\max})^2 \quad \forall i \in \widehat{\mathbf{N}}_a \quad (30)$$

$$\left\| \begin{matrix} 2P_{ij} \\ 2Q_{ij} \\ l_{ij} - v_i \end{matrix} \right\|_2 \le l_{ij} + v_i \quad \forall (i,j) \in \mathbf{E}_a \quad (31)$$

where, ns is the total number of sub-networks, $\widehat{\mathbf{N}}_a$ represents the nodes of sub-networks a excluding feeder, $\mathbf{N}_{DG,a}$ represents the set of nodes connecting with DGs inside sub-network a.

C. SOLUTION METHODOLGY

The primal variable is the original decision variable, which is updated thorough following,

$$\mathbf{x}_a^{k+1} = \arg\min_{\mathbf{x}_a} L_a(\mathbf{x}_a, \mathbf{u}_a^k, \boldsymbol{\lambda}_a^k) \quad (32)$$

where,$k+1$ represents the $(k+1)_{th}$ iteration, $\mathbf{u}_a^k, \boldsymbol{\lambda}_a^k$ represents the values of auxiliary variables and dual variables through the k_{th} iteration. Correspondingly, the auxiliary variable written through a simple pattern is shown as,

$$\mathbf{u}_{abi}^{k+1} = \frac{1}{2}(\mathbf{x}_{abi}^{k+1} + \mathbf{x}_{bai}^{k+1}) \quad (33)$$

The dual variable renewing equation is shown as,

$$\boldsymbol{\lambda}_{abi}^{k+1} = \boldsymbol{\lambda}_{abi}^{k} + \rho(\mathbf{x}_{abi}^{k+1} - \mathbf{u}_{abi}^{k+1}) \quad (34)$$

In accordance with alternating direction variable renew during iterations, the stopping criteria is also established based on the primal residual and the dual residual. The primal and dual residuals are represented by

$$\mathrm{r}^{k+1} = (\mathbf{x}_{ab1}^{k+1} - \mathbf{u}_{ab1}^{k+1}, \ldots, \mathbf{x}_{abnz}^{k+1} - \mathbf{u}_{abnz}^{k+1}) \quad (35)$$

$$s^{k+1} = -\rho(\mathbf{u}_{ab1}^{k+1} - \mathbf{u}_{ab1}^{k}, \ldots, \mathbf{u}_{abnz}^{k+1} - \mathbf{u}_{abnz}^{k}) \quad (36)$$

Then, the residuals norms are shown as

$$\left\|\mathbf{r}^{k+1}\right\|_2^2 = \sum_{i=1}^{nz} \left\|\mathbf{x}_{abi}^{k+1} - \mathbf{u}_{abi}^{k+1}\right\|_2^2 \quad (37)$$

$$\left\|\mathbf{s}^{k+1}\right\|_2^2 = ns \cdot \rho^2 \left\|\mathbf{u}_{abi}^{k+1} - \mathbf{u}_{abi}^{k}\right\|_2^2 \quad (38)$$

ADMM is sensitive to the penalty parameter, thus the penalty parameter is not set as fixed value but as varying

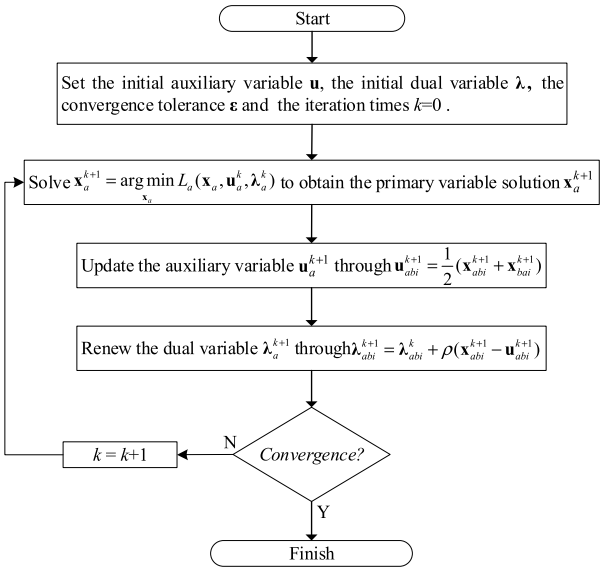

FIGURE 5. Flowchart of the ADMM solution method.

TABLE 1. Parameters of DGs in PG&E 69 test system.

Capacity	Forecasted Active Power	Locations
300 kVA	250 kW	5,17,25,36,46,50,54,65

parameter in this paper.

$$\rho^{k+1}=\begin{cases}\tau^{incr}\rho^k & \|\mathbf{r}^k\|_2^2>\mu\|\mathbf{s}^k\|_2^2\\ \rho^k/\tau^{decr} & \|\mathbf{s}^k\|_2^2>\mu\|\mathbf{r}^k\|_2^2\\ \rho^k & otherwise\end{cases}\tag{39}$$

where τ^{incr}, τ^{decr} and μ are the parameters greater than 1, and these parameters are set as $\tau^{incr}=\tau^{decr}=2$, $\mu=10$ in this paper.

ADMM achieves fast convergence through updating variables alternately during iterations, which is the reason of its named alternating direction method. The flowchart of the ADMM solution method is shown as in Fig. 5 and the procedure is as follows:

Procedure 1

1: **Initialization:**

Set the initial auxiliary variable $\mathbf{u}$, the initial dual variable λ, the convergence tolerance ε and the iteration times $k=0$.

2: **Local Optimization:**

The primary variable solution $\mathbf{x}_a^{k+1}$ is obtained through the local optimization shown as below,

$$\mathbf{x}_a^{k+1}=\arg\min_{\mathbf{x}_a} L_a(\mathbf{x}_a,\mathbf{u}_a^k,\boldsymbol{\lambda}_a^k)$$

3: **Auxiliary variable update:**

The auxiliary variable solution $\mathbf{u}_a^{k+1}$ is updated through by the following,

$$\mathbf{u}_{abi}^{k+1}=\frac{1}{2}(\mathbf{x}_{abi}^{k+1}+\mathbf{x}_{bai}^{k+1})$$

4: **Dual variable update:**

Renew the dual variable solution $\boldsymbol{\lambda}_a^{k+1}$ shown as,

$$\boldsymbol{\lambda}_{abi}^{k+1}=\boldsymbol{\lambda}_{abi}^{k}+\rho(\mathbf{x}_{abi}^{k+1}-\mathbf{u}_{abi}^{k+1})$$

5: **Check for convergence:**

If $\|\mathbf{r}^{k+1}\|_2^2\le\varepsilon^{pri}$ and $\|\mathbf{s}^{k+1}\|_2^2\le\varepsilon^{dual}$ terminate; otherwise set $k=k+1$ and go back to Step 2.

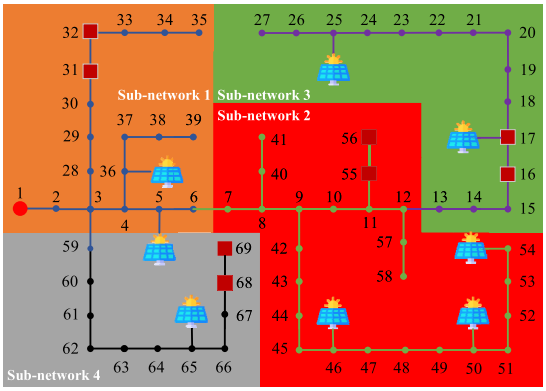

FIGURE 6. The topology of PG&E 69 bus system after partitioning.

IV. CASE STUDIES

The proposed two-stage D-ORPD is tested on the PG&E 69 bus test system [24] and the modified IEEE 123 bus test system [25]. The simulations are conducted by Matlab 2016 utilizing the commercial solver GUROBI on a laptop with 2.60 GHz CPU and 16.0 GB RAM.

A. NETWORK PARTITION OF PG&E 69 BUS TEST SYSTEM

In the PG&E 69 bus test system, 8 DGs are installed while the detailed data are shown in Table 1. The permitted voltage scope is set as [0.95, 1.05]. Based on the proposed DNs partitioning approach, the PG&E 69 bus system is separated into four different sub-networks. The topology of partitioned test system is shown in Fig. 6. It can be seen that network partitioning is not a simple "equal quality decomposition", such as 25 nodes in sub-network 1 while 9 nodes in sub-network 5, forming a distinctive comparison.

B. D-ORPD OF PG&E 69 BUS TEST SYSTEM

The iteration procedure is shown in Fig.7-Fig.9. From Fig.7, the primary residuals reached the convergence criterion (1e-4) after 62 times iterations while the dual residuals need 60 times iterations.

It shows the virtual active and reactive loads values during iterations in Fig.8. The VP 12 means the virtual active load between zone 1 and zone 2 from the side of zone 1 while VP 21 means the virtual active load between zone 1 and zone 2 from the side of zone 2. There is a similar way of naming

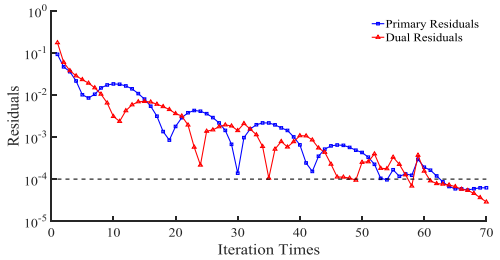

FIGURE 7. The primary and dual residuals during iterations of PG&E 69 bus system.

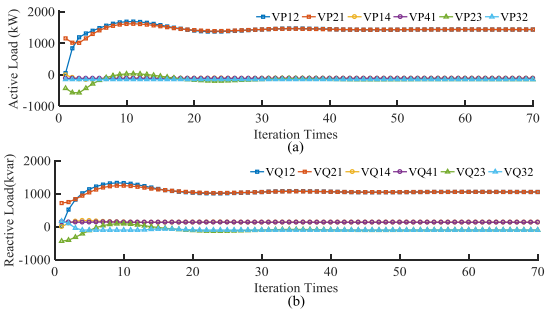

FIGURE 8. The virtual loads values during iterations of PG&E 69 bus system. (a) active virtual loads values; (b) reactive virtual loads values.

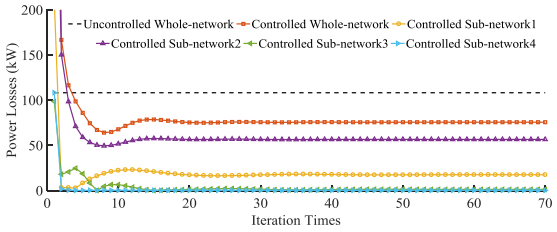

FIGURE 9. The uncontrolled and controlled power losses during iterations of PG&E 69 bus system.

for VP14, VP41, VP23 and VP32. It can be seen that after nearly 20 times iteration, each pair of the virtual load becomes unification. The power losses of the whole-network, sub-network 1, sub-network 2, sub-network 3 and sub-network 4 during iterations under D-ORPD are displayed in Fig. 9. Besides, the power losses without control are also shown in this figure. For the whole-network, the power losses reduce from 108 kW to 69 kW with a reduction of 36% applying D-ORPD.

C. NETWORK PARTITION OF IEEE123 BUS TEST SYSTEM

In this section, the balanced IEEE 123 bus test system is modified from the original unbalanced one. The voltage is limited in [0.95, 1.05], and the locations and capacities of 10 installed DGs are shown in Table 2. If without sub-network count setting, the system will be partitioned into 8 sub-networks while node 95 is set as one individual sub-network. However, this is not economical in practical ORPD. With the ideal amount of sub-networks is set as four, the whole system is partitioned into four sub-networks shown as in Fig. 10.

TABLE 2. Parameters of DGs in IEEE 123 bus test system.

Capacity	Forecasted Active Power	Locations
300 kVA	200 kW	27,30,41,44,51, 65,77,86,95,113

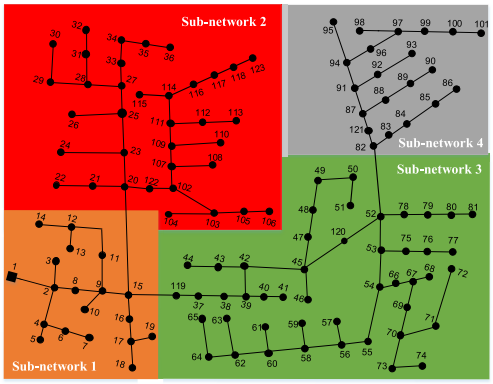

FIGURE 10. The topology of IEEE 123 bus system after partitioning.

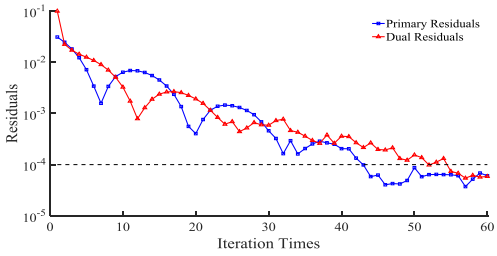

FIGURE 11. The primary and dual residuals during iterations of IEEE 123 bus system.

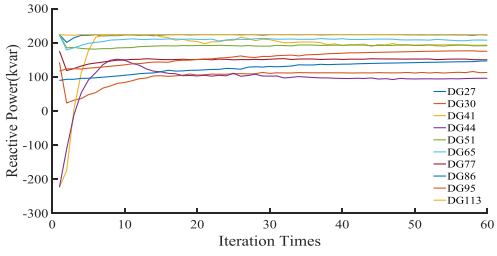

FIGURE 12. The reactive power output of DGs during iterations of IEEE 123 bus system.

D. D-ORPD OF IEEE123 BUS TEST SYSTEM

The primary and dual residuals during iterations are shown in Fig. 11. It can be seen that the D-ORPD converged fast while the needed iterations are less than 60 times. The reactive power supports of the 10 DGs during iterations are shown in Fig. 12.

The virtual load values during iterations are shown in Fig. 13 and it needs less than 10 times iterations for each pair of virtual loads to be consistent. The uncontrolled and controlled power losses during iterations are shown in Fig. 14.

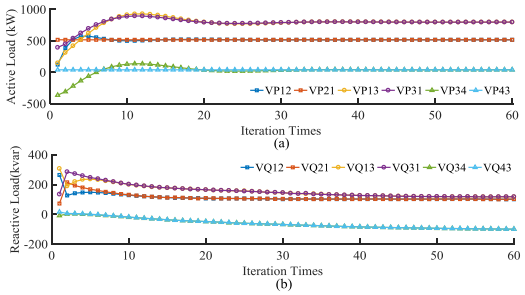

FIGURE 13. The virtual loads values during iterations of IEEE 123 bus system. (a) active virtual loads values; (b) reactive virtual loads values.

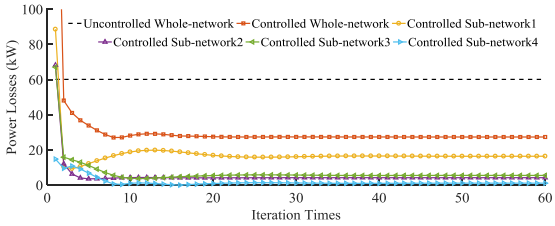

FIGURE 14. The uncontrolled and controlled power losses during iterations of IEEE 123 bus system.

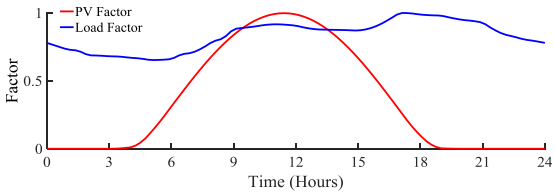

FIGURE 15. The PV and load factor in 24 hours.

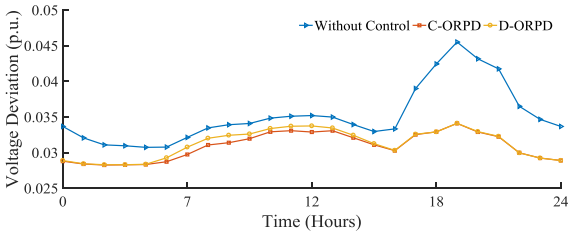

FIGURE 16. The voltage deviation of PG&E 69 bus system in 24 hours.

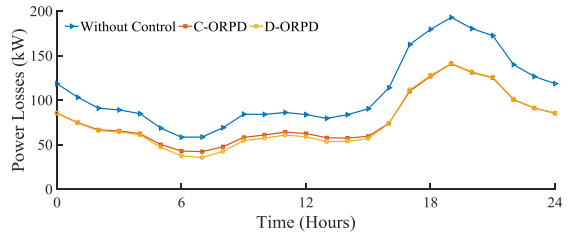

FIGURE 17. The power losses of PG&E 69 bus system in 24 hours.

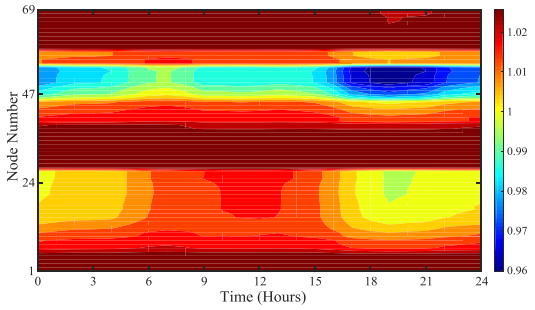

FIGURE 18. The voltage profile of PG&E 69 bus system in 24 hours.

For the controlled ones, not only the whole-network, but the power losses of each sub-network are also displayed. Applying D-ORPD, the power losses of the whole-network reduce from 60.15 kW to 24 kW with a reduction of 60.1%.

E. D-ORPD OF PG&E 69 SYSTEM ON 24 HOURS

The above test is only about the proposed method on a certain operating point. Aiming to verify the applicability and practicability of D-ORPD, the case study on varying condition scenario is conducted. PVs are selected as DGs, then the time-series load factor and PV's active power output factor are shown in Fig. 15.

From this load curve, there are two load demand peaks occurring on 11:00 am and 17:00 pm while the lowest load demand is on 5:00 am. The PVs' active power output meets the normal distribution. In 24 hours, the improvement of power quality and power losses are shown Fig. 16 and Fig. 17.

It can be seen that there is slight difference between D-ORPD and C-ORPD, which implies the high accuracy of D-ORPD. Besides, there is a large reduction in voltage deviations and power losses after applying the ORPD. Thus, this proposed approach is effective in both improving power quality and system operation economy. The voltage profile of the PG&E 69 system by applying D-ORPD is shown in Fig. 18. It can be seen that the voltage level of all the nodes are stable under a favorable level on most of the time in 24 hours.

V. CONCLUSION

A two-stage D-ORPD method has been proposed in this paper. On the first stage, the distribution network has been separated into several high intra-cohesiveness and low inter-coupling sub-networks so as to reduce the information communication and accelerate the distributed calculation. Based on the developed partition indexes, the BPSO has been utilized to divide the distribution network. On the second stage, the D-ORPD mathematical model in a "decomposition-coordination" architecture has been constructed. Furthermore, the virtual load which simulates the load characteristic of sub-networks has been proposed to enhance the consistency between distributed and centralized optimization. The ADMM has been employed to solve the distributed mathematical model. In addition, simulation has shown the fast convergence speed and reliable computation result of the two-stage D-ORPD.

REFERENCES

[1] Q. Li, Y. Zhang, T. Ji, X. Lin, and Z. Cai, "Volt/var control for power grids with connections of large-scale wind farms: A review," *IEEE Access*, vol. 6, pp. 26675–26692, 2018, doi: 10.1109/ACCESS.2018.2832175.

[2] K. Turitsyn, P. Sulc, S. Backhaus, and M. Chertkov, "Options for control of reactive power by distributed photovoltaic generators," *Proc. IEEE*, vol. 99, no. 6, pp. 1063–1073, Jun. 2011, doi: 10.1109/JPROC.2011.2116750.

[3] M. Farivar and S. H. Low, "Branch flow model: Relaxations and convexification—Part I," *IEEE Trans. Power Syst.*, vol. 28, no. 3, pp. 2554–2564, Aug. 2013, doi: 10.1109/TPWRS.2013.2255318.

[4] M. Farivar and S. H. Low, "Branch flow model: Relaxations and convexification—Part II," *IEEE Trans. Power Syst.*, vol. 28, no. 3, pp. 2565–2572, Aug. 2013, doi: 10.1109/TPWRS.2013.2255317.

[5] J. Lavaei and S. H. Low, "Zero duality gap in optimal power flow problem," *IEEE Trans. Power Syst.*, vol. 27, no. 1, pp. 92–107, Feb. 2012, doi: 10.1109/TPWRS.2011.2160974.

[6] H. Ahmadi, J. R. MartÃ, and H. W. Dommel, "A framework for volt-VAR optimization in distribution systems," *IEEE Trans. Smart Grid*, vol. 6, no. 3, pp. 1473–1483, May 2015, doi: 10.1109/TSG.2014.2374613.

[7] S. X. Chen, Y. S. F. Eddy, H. B. Gooi, M. Q. Wang, and S. F. Lu, "A centralized reactive power compensation system for LV distribution networks," *IEEE Trans. Power Syst.*, vol. 30, no. 1, pp. 274–284, Jan. 2015, doi: 10.1109/TPWRS.2014.2326520.

[8] S. Boyd, N. Parikh, E. Chu, B. Peleato, and J. Eckstein, "Distributed optimization and statistical learning via the alternating direction method of multipliers," *Found. Trends Mach. Learn.*, vol. 3, no. 1, pp. 1–122, Jan. 2011.

[9] E. Dall'Anese, H. Zhu, and G. B. Giannakis, "Distributed optimal power flow for smart microgrids," *IEEE Trans. Smart Grid*, vol. 4, no. 3, pp. 1464–1475, Sep. 2013, doi: 10.1109/TSG.2013.2248175.

[10] B. A. Robbins and A. D. Domínguez-García, "Optimal reactive power dispatch for voltage regulation in unbalanced distribution systems," *IEEE Trans. Power Syst.*, vol. 31, no. 4, pp. 2903–2913, Jul. 2016, doi: 10.1109/TPWRS.2015.2451519.

[11] C. Feng, Z. Li, M. Shahidehpour, F. Wen, W. Liu, and X. Wang, "Decentralized short-term voltage control in active power distribution systems," *IEEE Trans. Smart Grid*, vol. 9, no. 5, pp. 4566–4576, Sep. 2018, doi: 10.1109/TSG.2017.2663432.

[12] B. A. Robbins, H. Zhu, and A. D. Domínguez-García, "Optimal tap setting of voltage regulation transformers in unbalanced distribution systems," *IEEE Trans. Power Syst.*, vol. 31, no. 1, pp. 256–267, Jan. 2016, doi: 10.1109/TPWRS.2015.2392693.

[13] W. Zheng, W. Wu, B. Zhang, H. Sun, and Y. Liu, "A fully distributed reactive power optimization and control method for active distribution networks," *IEEE Trans. Smart Grid*, vol. 7, no. 2, pp. 1021–1033, Mar. 2016, doi: 10.1109/TSG.2015.2396493.

[14] B. A. Robbins, C. N. Hadjicostis, and A. D. Domínguez-García, "A two-stage distributed architecture for voltage control in power distribution systems," *IEEE Trans. Power Syst.*, vol. 28, no. 2, pp. 1470–1482, May 2013, doi: 10.1109/TPWRS.2012.2211385.

[15] B. Zhang, A. Y. S. Lam, A. Domínguez-García, and D. Tse, "An optimal and distributed method for voltage regulation in power distribution systems," *IEEE Trans. Power Syst.*, vol. 30, no. 4, pp. 1714–1726, Jun. 2015, doi: 10.1109/TPWRS.2014.2347281.

[16] A. Nedić, A. Olshevsky, and M. G. Rabbat, "Network topology and communication-computation tradeoffs in decentralized optimization," *Proc. IEEE*, vol. 106, no. 5, pp. 953–976, May 2018.

[17] K. Tsianos, S. Lawlor, and M. G. Rabbat, "Communication/computation tradeoffs in consensus-based distributed optimization," in *Proc. Adv. Neural Inf. Process. Syst.*, 2012, pp. 1943–1951.

[18] P. Lagonotte, J. C. Sabonnadiere, J. Y. Leost, and J. P. Paul, "Structural analysis of the electrical system: Application to secondary voltage control in France," *IEEE Trans. Power Syst.*, vol. 4, no. 2, pp. 479–486, May 1989, doi: 10.1109/59.193819.

[19] T. Kanungo, D. M. Mount, N. S. Netanyahu, C. D. Piatko, R. Silverman, and A. Y. Wu, "An efficient K-means clustering algorithm: Analysis and implementation," *IEEE Trans. Pattern Anal. Mach. Intell.*, vol. 24, no. 7, pp. 881–892, Jul. 2002, doi: 10.1109/TPAMI.2002.1017616.

[20] E. Cotilla-Sanchez, P. D. Hines, C. Barrows, S. Blumsack, and M. Patel, "Multi-attribute partitioning of power networks based on electrical distance," *IEEE Trans. Power Syst.*, vol. 28, no. 4, pp. 4979–4987, Nov. 2013.

[21] M. Nayeripour, H. Fallahzadeh-Abarghouei, E. Waffenschmidt, and S. Hasanvand, "Coordinated online voltage management of distributed generation using network partitioning," *Elect. Power Syst. Res.*, vol. 141, pp. 202–209, Dec. 2016, doi: 10.1016/j.epsr.2016.07.024.

[22] H. Mehrjerdi, S. Lefebvre, M. Saad, and D. Asber, "A decentralized control of partitioned power networks for voltage regulation and prevention against disturbance propagation," *IEEE Trans. Power Syst.*, vol. 28, no. 2, pp. 1461–1469, May 2013, doi: 10.1109/TPWRS.2012.2225154.

[23] J. Kennedy and R. C. Eberhart, "A discrete binary version of the particle swarm algorithm," in *Proc. IEEE Int. Conf. Syst., Man, Cybern. Comput. Simulation*, Orlando, FL, USA, vol. 5, Oct. 1997, pp. 4104–4108.

[24] J. S. Savier and D. Das, "Impact of network reconfiguration on loss allocation of radial distribution systems," *IEEE Trans. Power Del.*, vol. 22, no. 4, pp. 2473–2480, Oct. 2007.

[25] Y. Chai, L. Guo, C. Wang, Z. Zhao, X. Du, and J. Pan, "Network partition and voltage coordination control for distribution networks with high penetration of distributed PV units," *IEEE Trans. Power Syst.*, vol. 33, no. 3, pp. 3396–3407, May 2018.

PEISHUAI LI (SM'17) received the B.Eng. degree in automation engineering from Qingdao University, Qingdao, China, in 2010, and the M.Eng. degree in electrical power system and its automation form Shandong University, Jinan, China, in 2013. He is currently pursuing the Ph.D. degree in electrical engineering with Southeast University, Nanjing, China. From 2017 to 2018, was with the University of New South Wales as an Exchanging Student. His research interests include power system operation, security region estimation of active distribution networks, network partition, and distributed optimization.

ZAIJUN WU received the B.Eng. degree in power system and its automation from the Hefei University of Technology, Hefei, China, in 1996, and the Ph.D. degree in electrical engineering from Southeast University, Nanjing, China, in 2004. He was a Visiting Scholar with The Ohio State University, Columbus, OH, USA, from 2012 to 2013. He is currently a Professor with the School of Electrical Engineering, Southeast University. His research interests include substation automation, microgrid, and power quality. He is the author or coauthor of about 60 referred journal papers and a reviewer of several journals.

KE MENG received the Ph.D. degree from The University of Queensland, Australia, in 2009. He is currently with the School of Electrical Engineering and Telecommunications, University of New South Wales, Australia. He is also a Visiting Professor with the Changsha University of Science and Technology. His research interest includes power system stability analysis, power system planning, renewable energy, and power system data analytics.

GUO CHEN received the Ph.D. degree in electrical engineering from the University of Queensland, Brisbane, Australia, in 2010. He is currently an Australian Research Council Discovery Early Career Researcher Award Fellow and a Lecturer with the School of Electrical Engineering and Telecommunications, University of New South Wales, Sydney, Australia. He has also held academic positions at The Australian National University, The University of Sydney, and The University of Newcastle, respectively. His research interests include power system security assessment, optimization, and control, complex network, intelligent algorithms, and their applications in smart grid. He is an Editor of the IEEE TRANSACTIONS ON SMART GRID.

ZHAO YANG DONG (M'99–SM'06–F'17) received the Ph.D. degree from The University of Sydney, Australia, in 1999. He is currently a Professor and the Head with the School of Electrical and Information Engineering, The University of Sydney. He was the Ausgrid Chair and the Director of the Centre for Intelligent Electricity Networks, The University of Newcastle, Australia. He also held academic and industrial positions with The Hong Kong Polytechnic University and Transend Networks (now TASNetworks), Australia. His research interest includes smart grid, power system planning, power system security, renewable energy systems, electricity market, load modeling, and computational intelligence and its application in power engineering. He is an Editor of the IEEE TRANSACTIONS ON SMART GRID, the IEEE TRANSACTIONS ON SUSTAINABLE ENERGY, IEEE POWER ENGINEERING LETTERS, and *IET Renewable Power Generation*.